

Modulation of bay of bengal tropical cyclone activity by the madden-julian oscillation



Pankaj Bhardwaj^a, Omvir Singh^{a,*}, D.R. Pattanaik^b, Philip J. Klotzbach^c

^a Department of Geography, Kurukshetra University, Kurukshetra 136119, India

^b India Meteorological Department, Mausam Bhawan, Lodhi Road, New Delhi 110003, India

^c Department of Atmospheric Science, Colorado State University, Fort Collins, CO, USA

ARTICLE INFO

Keywords:
 Madden-Julian oscillation
 Tropical cyclones
 Convective activity
 Environmental conditions
 Bay of Bengal

ABSTRACT

The influence of the Madden-Julian oscillation (MJO) on global tropical cyclone (TC) activity has been well documented in many earlier studies. However, no prior studies have focused specifically on the MJO's impacts on TCs in the Bay of Bengal (BoB). Therefore, the present study examines the impact of the MJO on BoB TC activity during the two peak TC periods i.e. April–June (AMJ) and October–December (OND) from 1974 to 2015. The MJO considerably modulates various measures of TC activity in the BoB, including the number of TCs, the number of TC days, accumulated cyclone energy, the power dissipation index, TC genesis location and TC tracks. TC activity is significantly enhanced (suppressed) over the BoB when the convectively active MJO phase is positioned over the eastern Indian Ocean and the Maritime Continent (the Western Hemisphere and Africa). Alterations in the TC genesis locations and their tracks are more pronounced in OND than in AMJ. These changes in TC characteristics are mainly attributed to MJO-driven modulations in large-scale environmental conditions such as deep convection, mid-tropospheric relative humidity, sea surface temperature, sea level pressure, lower- and upper-level winds and vertical wind shear. A comprehensive knowledge of the MJO-TC relationship may be beneficial for short-term predictions of TC activity in the BoB.

1. Introduction

The Madden-Julian oscillation (MJO) is a dominant mode of tropical intraseasonal variability with a time-scale of approximately 30–60 days (Madden and Julian, 1972, 1994). It is characterized by a global scale eastward-moving deep convective region which is usually bounded by two suppressed convective regions on its eastern and western sides (Madden and Julian, 1971; Zhang, 2005; Zhou and Chan, 2005). The enhanced and suppressed convective anomalies are mainly found between the Indian Ocean and 180° longitude (Matthews, 2000), whereas the circulation anomalies can propagate around the tropics (Krishnamurti et al., 1985). These convectively-enhanced and suppressed MJO phases considerably modulate TC activity, monsoon and precipitation patterns, as well as other extreme weather events for various portions of the globe (Goswami and Ajayamohan, 2001; Jones and Carvalho, 2002; Lorenz and Hartmann, 2006; Thompson and Roundy, 2013; Jones and Carvalho, 2014; Marzuki et al., 2016; Bhatia et al., 2017; Mandapaka et al., 2017; Wang and Moon, 2017a; Zaitchik, 2017; Shao et al., 2018; Anandh et al., 2018; Notaro, 2018).

Furthermore, it has been well documented that convectively active

and inactive phases of the MJO result in enhanced and suppressed TC activity, respectively, for various global TC basins (Camargo et al., 2009; Klotzbach, 2014). Gray (1979) noted that TCs form in clusters, with alternating enhanced and suppressed periods. Later, Nakazawa (1986) used data from 1979 and found that TC formation was usually above-average (below-average) with convectively active (inactive) phases spanning a period of 30–60 days. Liebmann et al. (1994) demonstrated a significant increase in TC formation in the western North Pacific and in the Indian Ocean that tended to cluster around low-level cyclonic vorticity and upper-level divergence anomalies occurring during the convectively active phase of the MJO.

Recently, several researchers have demonstrated a link between the MJO and TCs around the globe. Camargo et al. (2009) found that positive genesis potential anomalies are consistent with the regions of enhanced TC genesis frequency, which tend to be centered slightly poleward and a little westward of the center of the convective envelope of the MJO. Klotzbach (2014) showed that TC activity is usually enhanced during and immediately following the active convective phase of the MJO, and TC activity is usually suppressed during and immediately following the convectively suppressed phase. Similarly,

* Corresponding author.

E-mail addresses: ovshome@yahoo.com, osingh@kuk.ac.in (O. Singh).

Klotzbach and Oliver (2015a) showed that the periods of enhanced TC activity are associated with periods when the convectively active portion of the MJO passes over a specific basin. Wang and Moon (2017) observed that the MJO-induced off-equatorial low-level cyclonic (anticyclonic) vorticity anomalies generate upward (downward) motion and moisten (dry) the lower troposphere, thereby enhancing (suppressing) TC genesis.

In the North Atlantic basin, Mo (2000) demonstrated that TCs are most likely to develop in the Atlantic when enhanced convection is located over the Indian Ocean and convection in the central Pacific is suppressed. Maloney and Hartmann (2000a) showed that TC formation in the Gulf of Mexico and western Caribbean occurs about four times more often when low-level wind anomalies in the Eastern Pacific driven by the MJO are westerly than when they are easterly. The enhancement of TC genesis during westerly MJO periods accompanies cyclonic wind anomalies over the Gulf of Mexico, western Caribbean and tropical Atlantic. Klotzbach (2010) and Ventrice et al. (2011) showed that TC activity in the Atlantic Main Development Region increases when enhanced convection is located over Africa and the western Indian Ocean. The likelihood for rapid intensification of TCs also increased when enhanced convection driven by the MJO is in the Indian Ocean (Klotzbach, 2012). Klotzbach and Oliver (2015b) showed that TC activity in the Atlantic basin increases when MJO-related convection is enhanced over Africa and the Indian Ocean, while it decreases when the MJO enhances convection over the western Pacific.

In the western North Pacific, TC genesis is more frequent during the active MJO phase than during the suppressed phase (Liebmann et al., 1994; Sobel and Maloney, 2000; Kim et al., 2008; Huang et al., 2011; Li and Zhou, 2013a, 2013b; Li and Zhou, 2018). The westerly phase of the tropical intraseasonal oscillation is much more favorable for TC genesis than during the easterly phase (Maloney and Dickinson, 2003; Kim et al., 2008; Ko and Hsu, 2009). Kim et al. (2008) also showed that TC tracks migrate eastward (westward) when MJO-related convection is located in the equatorial Indian Ocean (tropical western North Pacific). Li et al. (2012) showed that during the active MJO phase, strong low-level westerlies strengthen the monsoon trough, which leads to enhanced cyclonic vorticity, increased relative humidity and anomalous rising motion in the western North Pacific that are favorable for TC formation. Zhao et al. (2015) confirmed that there are large positive anomalies of the genesis potential index during the active phase of the MJO. They found that mid-level relative humidity and low-level relative vorticity are the two largest contributors towards the positive genesis potential index anomalies during the active MJO phase. Chen et al. (2018) showed that the productivity of TC genesis increases (decreases) during the active (inactive) MJO phase.

In the eastern North Pacific, Molinari et al. (1997) examined the 13 TCs that formed in 1991 and found a correlation between eastern North Pacific TC genesis and the strength of a potential vorticity gradient in the Caribbean Sea. They attributed this relationship to the enhancement of westward-propagating tropical waves by the MJO. Molinari and Vollaro (2000) studied eastern North Pacific TC formation for the 1991 season, and observed that TCs tend to form progressively eastward with the eastward propagation of the MJO. Maloney and Hartmann (2000b) demonstrated that TC activity in the eastern North Pacific Ocean increases significantly when MJO-associated low-level westerly wind anomalies prevail in the basin. Aiyer and Molinari (2008) showed that TC genesis is enhanced in the eastern North Pacific with the passage of the convectively-enhanced phase of the MJO over the basin. Barrett and Leslie (2009) showed an increase in TC genesis in the eastern North Pacific when upper-level divergence is located near 120°W. Klotzbach and Blake (2013) studied TC activity over the central North Pacific (west of 120°W) and observed that enhanced convection linked with the MJO over the eastern and central Pacific results in an increase in TC development in the central North Pacific.

Hall et al. (2001) showed that the MJO strongly modulates the pattern of TC formation in the Southern Hemisphere between the

longitudes of 80° and 170°E, in accordance with large-scale variations in 850 hPa relative vorticity. Bessafi and Wheeler (2006) observed that favorable low-level vorticity and vertical shear anomalies favor enhanced TC formation in the south Indian Ocean during the convectively-active MJO phase. Ho et al. (2006) showed that there were more frequent TC formations in the south Indian Ocean when enhanced convection is located in the Indian Ocean and also found that the area of enhanced TC formation moved eastward with the eastward shift of the MJO. Chand and Walsh (2010) found that TC formation during the active MJO phase is approximately five times more than during the inactive MJO phase near Fiji. Low-level cyclonic relative vorticity, upper-level divergence, and weak vertical wind shear provide favorable conditions for enhanced TC genesis in the active phase of the MJO. Ramsay et al. (2012) performed a cluster analysis of TCs in the Southern Hemisphere and found that the MJO enhances South Indian TC genesis when the MJO favors convective enhancement in the same region. South Pacific TC activity is favored when MJO-enhanced convection is located over the western Pacific and the Western Hemisphere. Maru et al. (2018) showed that more frequent TC activity occurs around the Solomon Islands when the MJO is located over the western Pacific Ocean and the Western Hemisphere due to the presence of strong convective activity and low-level negative background relative vorticity.

The North Indian Ocean, including the BoB and the Arabian Sea, accounts for just 7% of global TCs on average (Neumann, 1993). About 80% of North Indian Ocean TCs form in the BoB, and they tend to be the most deadly of any TCs around the globe (IMD, 2011). Adjoining coastal countries including Bangladesh, India and Myanmar reported > 75% of the casualties caused by BoB TCs (Chowdhury, 2002). Hence, a comprehensive analysis of BoB TCs from an MJO perspective can be beneficial in both understanding their occurrence and minimizing their deadly effects. Kikuchi and Wang (2010), Krishnamohan et al. (2012), Tsuboi and Takemi (2014) and Girishkumar et al. (2015) investigated the TC relationship with the MJO over the North Indian Ocean and showed that TC development was favored when enhanced convection occurred over the eastern Indian Ocean and the Maritime Continent. However, these studies were limited in the time span investigated, and there was a lack of discussion on the modulation of TC genesis locations and tracks by the MJO. Moreover, no study, to the authors' knowledge, has specifically focused on the MJO's impacts on BoB TCs.

This study, therefore, explores the association between BoB TC activity and the MJO over a longer time period (1974–2015, excepting 1978). This study also seeks to understand the MJO-driven modulations in large-scale environmental conditions over the BoB. The remainder of this paper is organized as follows: section 2 describes the datasets and the methods employed. Section 3 discusses the main results, including the MJO's relationship with TC frequency and distribution as well as the MJO-forced alterations in large-scale environmental conditions over the BoB. Section 4 summarizes the main findings of this study.

2. Database and methodology

2.1. MJO index

For the present study, daily real-time multivariate MJO (RMM) index data has been obtained from the Bureau of Meteorology website (<http://www.bom.gov.au/climate/mjo/>) to identify the phase and amplitude of the MJO for the period 1974–2015, except 1978 when outgoing long wave radiation (OLR) observations were unavailable (Wheeler and Hendon, 2004). Satellite OLR data first became available in 1974. This RMM index is based on the first two empirical orthogonal functions (EOFs) (RMM1 and RMM2) of the combined fields of equatorially-averaged (15°S–15°N) OLR, 850 and 200 hPa zonal wind data. The first two principal components (PCs) of the first two EOFs are termed real-time multivariate MJO series 1 (RMM1) and real-time

multivariate MJO series 2 (RMM2). RMM1 and RMM2 have been used to identify two fundamental characteristics of the MJO: phase (P) and amplitude. These two can be computed as:

$$\text{Amplitude} = \sqrt{\text{RMM1}^2 + \text{RMM2}^2} \quad (1)$$

$$\text{Phase } (\theta) = \tan^{-1} \frac{\text{RMM2}}{\text{RMM1}} \quad (2)$$

Wheeler and Hendon (2004) divided the entire MJO cycle on the basis of the phase angle into eight phases. In these eight phases, phase 2 and 3 (P2 and P3) represent enhanced convection over the Indian Ocean, P4 and P5 represent enhanced convection over the Maritime Continent, P6 and P7 represent enhanced convection over the western Pacific Ocean, and P8 and P1 represent enhanced convection over the Western Hemisphere and Africa. They defined an active MJO day when the amplitude value was > 1 . Many researchers have used the same definition to define an active MJO day. However, in the present study, a day is considered as an active MJO day when the amplitude is ≥ 0.75 . We have used a more relaxed active MJO amplitude definition in order to accommodate more TC formations given the fairly small sample size of Bay of Bengal TCs. All of those days when the amplitude value is smaller than 0.75 have been included in an additional phase called the 'weak phase'. The TCs have been grouped into eight MJO phases by using the cyclogenesis date. The cyclogenesis date is defined as the first day that the TC is classified as a tropical depression. If a TC underwent cyclogenesis in phase 1, aggregate statistics for that TC were counted in phase 1, regardless if the MJO progressed into other phases during the TC's lifetime.

2.2. Tropical cyclone data

Joint Typhoon Warning Center (JTWC) best track data for the period 1974–2015 (except for 1978 as the MJO data is unavailable for that year) have been utilized in this study (Chu et al., 2002). The dataset includes: the TC's name, its position (latitude and longitude), its minimum sea level pressure and its 1-min maximum sustained wind (MSW) speed at 6-h intervals (0000, 0600, 1200, and 1800 UTC). This data has been classified into different categories on the basis of maximum sustained wind speed (MSW) following the classification of the India Meteorological Department: low pressure area (L; < 17 knots), depression (D; 17–27 knots), deep depression (DD; 28–33 knots), cyclonic storm (CS; 34–47 knots), severe cyclonic storm (SCS; 48–63 knots), very severe cyclonic storm (VSCS; 64–89 knots), extremely severe cyclonic storm (ESCS; 90–119 knots) and super cyclonic storm (SupCS; ≥ 120 knots). The weakest three categories (when MSW is < 34 knots) have been excluded from the scope of the present study. We have focused only on the CS and more intense categories (when MSW is ≥ 34 knots). If a system reaches CS intensity at some point during its lifetime, it is considered as a TC. To calculate the number of TC days, the total number of six-hourly periods where a TC is of CS or greater intensity have been divided by 4 and summed for the season.

2.3. Tropical cyclone energy metrics

Two frequently used TC energy metrics are accumulated cyclone energy (ACE) (Bell et al., 2000) and the power dissipation index (PDI) (Emanuel, 2005). These indices have been computed to characterize overall TC activity in the BoB. ACE is defined as $\text{ACE} = \Sigma V_{\max}^2$ and has units of 10^4 kt^2 , where V_{\max} is the MSW of the TC. ACE is the sum of V_{\max} squared for all six-hourly periods when the MSW is ≥ 34 knots during the lifetime of a TC. The annual ACE has been calculated by summing up the ACE of all TCs in a year. PDI, defined as $\text{PDI} = \Sigma V_{\max}^3$, has units of 10^6 kt^3 and has been used to characterize the destructive potential of TCs. Both energy metrics take into account the frequency, intensity and duration of all of the TCs in a season.

2.4. Large scale environmental parameters

The relationship between large scale environmental conditions and TC activity is well recognized (Gray, 1968, 1979; McBride and Zehr, 1981; Frank, 1987; Merrill, 1988; Landsea et al., 1998). Gray (1968, 1975, 1979) observed that pre-existing dynamic and thermodynamic environmental conditions were vital for the formation of TCs. In this study we investigate changes in OLR, relative humidity (RH), sea surface temperature anomalies (SSTAs), sea level pressure (SLP), and 200 and 850 hPa zonal (U) winds to determine how these large-scale oceanic and atmospheric conditions are modified over the BoB by the MJO. Composites have been constructed using daily data from the National Centers for Environmental Prediction-National Center for Atmospheric Research (NCEP-NCAR) reanalysis (Kalnay et al., 1996).

2.5. Statistical test

A z-test, following Hall et al. (2001), has been applied to identify whether TC activity is significantly enhanced or suppressed in a particular MJO phase. Here, TC activity is measured using four metrics: the number of TCs (TCN), the number of TC days (TCD), ACE and PDI. The null hypothesis is that TC activity occurs equally during each MJO phase, that is, there is no modulation of TC activity by the MJO. The relevant z-test has been computed separately for each category as follows:

$$Z = \frac{\hat{p}_e - p_e}{\sqrt{p_e(1-p_e)/N}} \quad (3)$$

where, \hat{p} and p_e are the observed and expected fractions of TC activity for each MJO phase, respectively, and N represents the number of days in each category. The expected fraction is computed by dividing the TC activity by the total number of days. The two-tailed test has been applied at the 90% and 95% confidence levels, with critical values of $Z = \pm 1.64$ and $Z = \pm 1.96$, respectively. When referring to significant TC modulation by the MJO, all results are listed at the 95% confidence level unless otherwise noted.

Additionally, a Monte Carlo bootstrap resampling technique has been applied to assess the significance level of the mean MJO modulation for each environmental parameter (Efron, 1979). A total of the number of days that the MJO amplitude was ≥ 0.75 in each phase was selected randomly with replacement from the full sample. This process was repeated 1000 times, and the obtained results were then sorted. The 5% and 95% confidence levels were determined from the 50th and 950th of the 1000 random samples.

A ratio of the maximum to the minimum normalized TC activity, called the enhancement to the suppression ratio (ESR), of different MJO phases has also been computed to detect the strength of the MJO-TC activity modulation (Li et al., 2012). Larger ESR values indicate a larger modulation of TC activity by the MJO.

3. Results and discussion

3.1. TC climatology

Here we briefly discuss the TC climatology over the BoB before delving further into the MJO-TC relationship. Fig. 1 displays a bimodal pattern in the occurrence of TCs over the BoB during 1974–2015 (excluding 1978). A total of 132 TCs formed in the BoB during the 41-year time period. Out of the 132 TCs, 95 (~72%) formed when the MJO amplitude was ≥ 0.75 . The maximum number of TCs formed during November followed by October, May and then December. No TCs formed during either February or August. The two TC periods, October–December (OND; 59 TC (~62%)) and April–June (AMJ; 27 TCs (~28%)) accounted for $> 90\%$ of the total number of TCs (when the MJO amplitude ≥ 0.75). Therefore, the present study seeks to explore

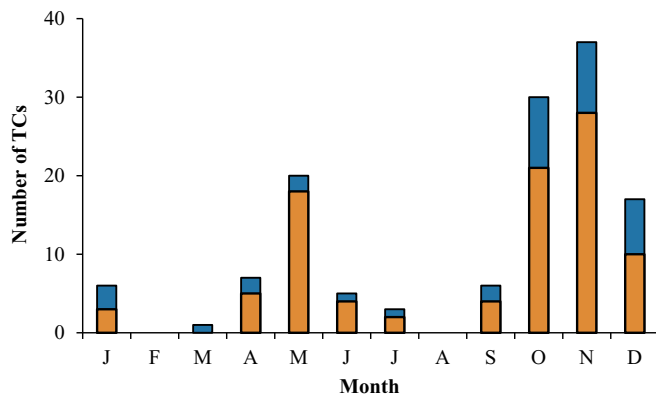


Fig. 1. Monthly distribution of TCs over the BoB during 1974–2015 (excluding 1978). The blue bar represents the total number of TCs, whereas the brown bar represents the number of TCs when the MJO amplitude is ≥ 0.75 . (For interpretation of the references to colour in this figure legend, the reader is referred to the web version of this article.)

the impact of the MJO on the AMJ and OND TC periods separately.

3.2. MJO versus TCs frequency

Fig. 2a displays a phase space diagram for the AMJ period denoting the distribution of TCs during different MJO phases. Of the total 3670 days in the AMJ period (41 years), only 32 days are associated with cyclogenesis. Hence, the average daily probability of TC formation over the BoB during the AMJ is $\sim 0.9\%$. A total of 27 of the 32 TCs ($\sim 82\%$) formed during active MJO days in the AMJ period. Three phases, P2 (13%), P3 (25%) and P4 (25%) accounted for $\sim 63\%$ of the TCs that formed in the AMJ period, while the remaining five phases (P1, P5–P8) accounted for the remaining 21% of TCs that formed. Interestingly, no TCs from 1974 to 2015 formed during AMJ in P8.

The corresponding statistics related to TC activity are shown in

Table 1. In this table, column 2 displays the number of days that the MJO spent in different phases over the BoB. Columns 3, 5, 7 and 9 show the total number of TCs, TCD, ACE and PDI, respectively, and columns 4, 6, 8 and 10 show their normalized values. The number of TCs, TCD, ACE and PDI have been normalized since the MJO can spend more time in certain phases than in others (Ventrice et al., 2011; Klotzbach, 2012). TC formations in the BoB are significantly enhanced during P3 and P4 whereas TC formation is significantly suppressed (at the 90% confidence level) in P8. Similarly, TCD are significantly enhanced in P3 and P4 and suppressed in P7, P8 and P1. The values of ACE and PDI are also significantly higher in P2, P3 and P4 and lower in P7, P8 and when the MJO is weak. These statistics on normalized TC formation produce an enhancement to suppression ratio in the normalized TC number of about 9 (P3) to 1 (P7) over the BoB. This indicates that TCs are about 9 times more likely to form in P3 than in P7 over the BoB during the AMJ period. The enhancement to suppression ratio of normalized TCD, ACE and PDI is 13, 15 and 19, respectively. We also note that since no TCs have formed in P8, the enhancement to suppression ratio for that MJO phase is undefined.

Fig. 2b displays phase space diagram indices for the OND period to denote the distribution of TCs during different MJO phases. Of the total 3772 days in the OND period (41 years), 84 days are associated with cyclogenesis, hence, the average probability of TC formation over the BoB is 2.2% during this period. The TC formation rate in the BoB is about three times higher in OND than in AMJ. Approximately 73% of OND TCs formed during active MJO days. The frequency of TCs is higher in P2 (12%), P3 (11%), P4 (14%) and P5 (13%) than in other phases, although these increases are statistically insignificant (Table 1). From this it can be inferred that the MJO does not significantly modulate TC frequency during OND. However, TCD, ACE and PDI are significantly modulated by the MJO over BoB. The TCD are significantly higher in P2 and P4 and lower in P6 and P7. The ACE and PDI values are significantly higher in P2, P4 and P5 and lower in P1 and P7. These statistics on normalized TC formation produce an enhancement to suppression ratio of about 3 (P4) to 1 (P7) over the BoB. This indicates

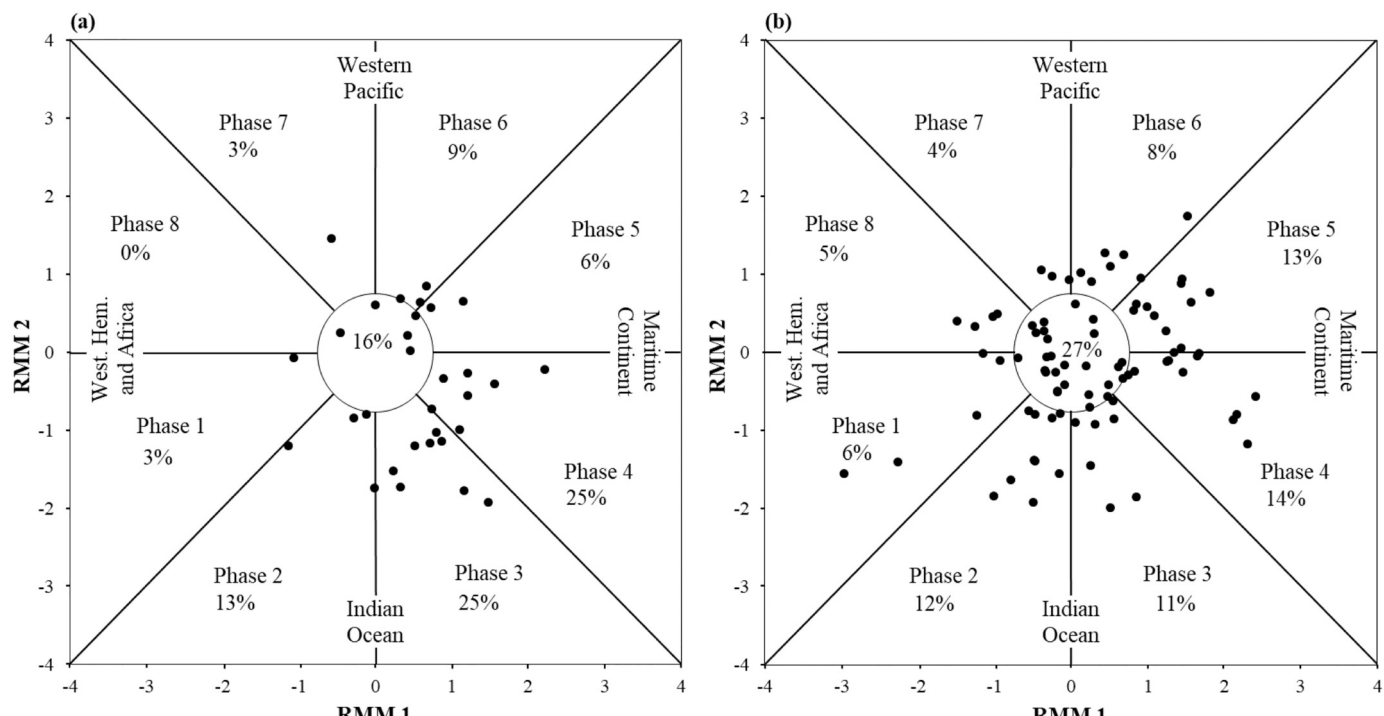


Fig. 2. The relationship between TC genesis and MJO phase during (a) AMJ and (b) OND from 1974 to 2015 (excluding 1978). The phase amplitude diagram is constructed with the principal components RMM1 and RMM2 of the MJO. The black dots represent days where TC genesis occurred. The circle in the center with an amplitude of 0.75 represents the days with weak MJO activity.

Table 1

The number of days in each MJO phase, the TCN (the number of TCs), the TCD (the number of TC days), ACE (10^4kt^2) and PDI (10^6kt^3) along with their normalized values (probability) generated by all TCs during 1974 to 2015 (except 1978). Normalized values (in %) are calculated by dividing the TC activity by the number of days spent in each phase and then multiplying by 100. This provides the level of TC activity that would be expected for 100 days in a particular MJO phase. Phases in which TC activity are significantly enhanced (suppressed) at the 90% and 95% significance levels are indicated by * and ** (+ and ++), respectively.

MJO Phase	MJO days	TCN	TCN (%)	TCD	TCD (%)	ACE	ACE (%)	PDI	PDI (%)
AMJ									
1	401	1	0.25	7.00	1.75 ⁺⁺	9.86	2.46 ⁺	9.30	2.32
2	361	4	1.11	20.75	5.75	22.60	6.26**	19.46	5.39**
3	304	8	2.63**	52.50	17.27**	38.19	12.56**	23.36	7.68**
4	350	8	2.29**	49.25	14.07**	38.47	10.99**	30.60	8.74**
5	325	2	0.62	9.75	3.00 ⁺	5.44	1.67 ⁺⁺	2.71	0.83 ⁺⁺
6	342	3	0.88	16.00	4.68	13.20	3.86	8.89	2.60
7	350	1	0.29	4.50	1.29 ⁺⁺	2.91	0.83 ⁺⁺	1.58	0.45 ⁺⁺
8	358	0	0.00 ⁺	0.00	0.00 ⁺⁺	0.00	0.00 ⁺⁺	0.00	0.00 ⁺⁺
Weak MJO	879	5	0.57	25.50	2.90 ⁺⁺	23.83	2.71 ⁺⁺	20.44	2.32
Total	3670	32	0.87	185.25	5.05	154.49	4.21	116.34	3.17
OND									
1	303	5	1.65	43.5	14.36	16.82	5.55 ⁺⁺	10.33	3.41 ⁺⁺
2	360	10	2.78	77.75	21.60**	53.44	14.84**	35.48	9.86**
3	383	9	2.35	46.75	12.21	30.69	8.01	19.95	5.21
4	394	12	3.05	65.5	16.62*	53.74	13.64**	43.17	10.96**
5	417	11	2.64	58	13.91	49.27	11.81**	38.85	9.32**
6	361	7	1.94	32.25	8.93 ⁺⁺	32.64	9.04	32.12	8.90
7	328	3	0.91	19.5	5.95 ⁺⁺	6.23	1.90 ⁺⁺	2.85	0.87 ⁺⁺
8	279	4	1.43	39.75	14.25	26.16	9.38	20.16	7.22
Weak MJO	947	25	2.64	144.25	15.23	82.76	8.74	59.89	6.32
Total	3772	84	2.23	515.75	13.67	341.07	9.04	255.43	6.78

that TCs form about 3 times more in P4 than P7 over BoB during the OND period. Similarly, the enhancement to suppression ratio of normalized TC numbers, ACE and PDI are 4, 8 and 13, respectively. This indicates that the influence of the MJO is more on AMJ TC activity than on OND TC activity. The enhancement to suppression ratio is almost double in AMJ what it is in OND, although this could be the result of the small sample size. These results of the MJO's impacts on TCs are consistent with previous studies investigating the impact of the MJO on North Indian Ocean TCs (Krishnamohan et al., 2012; Klotzbach, 2014). Since the number of TCs are fewer in the BoB than in most other ocean basins, results of statistical tests should be interpreted cautiously.

Fig. 3 displays the frequency distribution of TCs of different

categories, ACE and PDI in each MJO phase during the AMJ and OND periods. The rate of change of CSs (MSW 34–47 knots) to intense cyclones (MSW ≥ 48 knots) is higher in AMJ than in OND. Most ESCS and SupCS formed when the convectively-enhanced MJO phase is located over the eastern Indian Ocean and the Maritime Continent. Likewise, Klotzbach (2014) showed that the number of named storms, hurricanes and major hurricanes (using US definitions for TC intensity) were significantly higher in P4 and P5 over the North Indian Ocean. Like TC frequency, ACE and PDI values are also significantly higher in P2 to P4 (AMJ) and P2, P4 and P5 (OND). We find that TC formation is slightly less in P3 during OND. Most cyclogenesis occurs in the southwestern parts of the BoB, and TCs tend to travel short distances prior to landfall, therefore, the likelihood for them to make landfall before reaching TC intensity (i.e. ≥ 34 knots) is quite high (Fig. 4). Krishnamohan et al. (2012) also showed that there were fewer TCs in P3 compared to P2 and P4 during OND. The duration of TCs and their ACE and PDI values are also small in P3, as they travelled short distances after genesis with less chance to intensify (Table 1).

3.3. MJO versus TC genesis location and TC track

The MJO significantly modulates the genesis locations, tracks and landfall locations of TCs (Li and Zhou, 2013b). Fig. 4 displays the spatial distribution of TC genesis location along with TC tracks during AMJ and OND over the BoB. The figure demonstrates that the MJO significantly modulates TC genesis location and track during both AMJ and OND over the BoB. During AMJ, TC frequency is much less in P1, P5, P6, P7, and no TCs formed in P8. In P2, most TCs formed in the northeastern part of the BoB. The genesis locations then shifts towards the central to southwestern parts of the BoB in P3 and P4. Afterward, the TC genesis location again shifts northward from P5. The TCs that formed in the southern part of the BoB typically took westward to northwestward tracks. However, most TCs that formed in the central to northern part of the BoB followed a northward track after genesis and made landfall along the Bangladesh and Myanmar coasts (Fig. 4a).

During OND (Fig. 4b), TC frequency is higher than in AMJ in each MJO phase. Also, the MJO appears to modulate both TC genesis location and TC track during this period. TC landfalls occur over eastern India as well as along the Bangladesh and Myanmar coasts. Most TCs

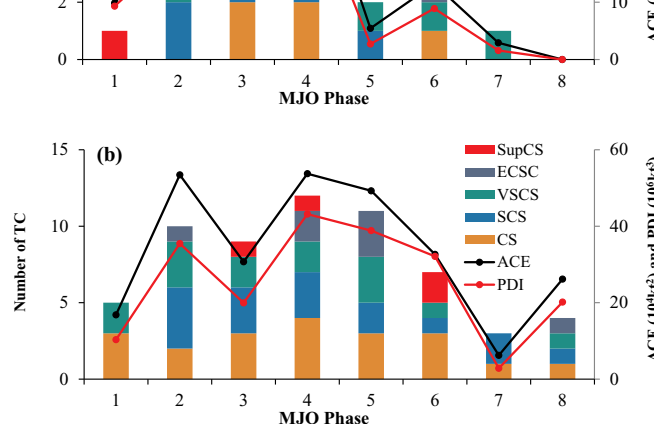


Fig. 3. The number of TCs of each intensity category, as well as ACE and PDI values in (a) AMJ and (b) OND in each MJO phase (when amplitude is ≥ 0.75) over the BoB from 1974 to 2015 (excluding 1978).

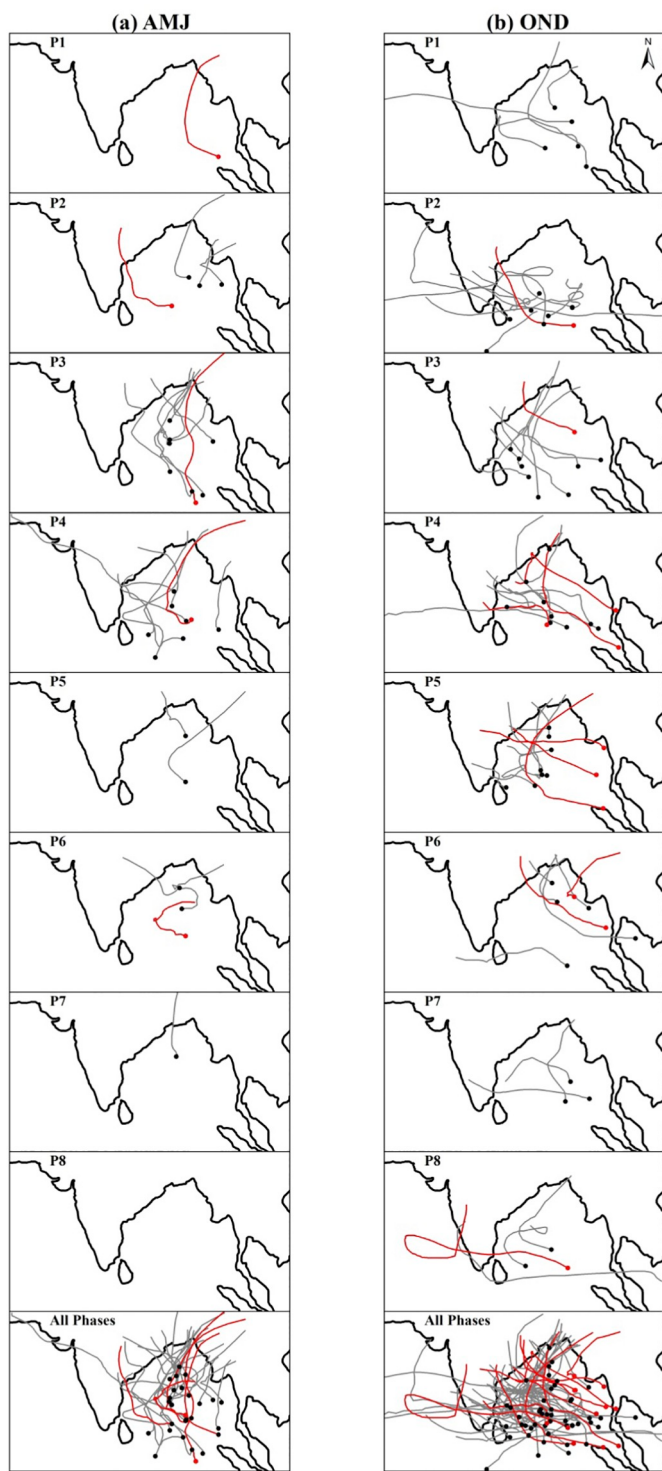


Fig. 4. Genesis location (dots) and tracks (lines) of TCs in each MJO phase (when amplitude is ≥ 0.75) during (a) AMJ and (b) OND periods from 1974 to 2015 (excluding 1978). Red colored dots and lines represent the genesis location and tracks of ESCSs and SupCSs, respectively. (For interpretation of the references to colour in this figure legend, the reader is referred to the web version of this article.)

take westward tracks after genesis in P2. TCs forming in P3 to P6 tend to take north-westward or northward tracks. Also, the genesis location tended to shift northward from P3 to P6. The TC genesis location then shifts southwards from P7 to P3. Most CSs which reached ESCS and SupCS intensity formed over the eastern or southeastern part of the BoB

(Fig. 4). These CSs tend to travel long distances prior to landfall, therefore allowing them ample time over very warm sea surface temperatures to strengthen into ESCSs and SupCSs.

It is important to note that the MJO modulates TC genesis location and track during both AMJ and OND, although the modulation is clearer during the latter period. Given the small number of TCs in AMJ, it is more difficult to draw clear conclusions about TC tracks during AMJ than during OND.

3.4. MJO modulation of large scale environmental conditions

In this section, we discuss the impact of the MJO on several key environmental parameters: upper- and lower-level zonal winds, relative humidity (RH), sea level pressure (SLP), vertical wind shear (VWS), OLR and SST (Pattanaik and Rama Rao, 2009; Klotzbach, 2010; Chand and Walsh, 2010; Kikuchi and Wang, 2010; Bhardwaj et al., 2019). Accordingly, the anomaly composites of these parameters have been constructed for the AMJ and OND periods during the eight MJO phases when the amplitude was ≥ 0.75 . All of the anomalies are calculated from a 1981–2010 climatology.

3.4.1. Outgoing longwave radiation (OLR)

Fig. 5 displays the OLR anomaly pattern corresponding to the eight MJO phases for both the AMJ and OND periods. Negative (positive) OLR anomalies indicate enhanced (suppressed) convection over a region. The region of enhanced convection follows the suppressed convection for the complete life cycle of the MJO. During AMJ (Fig. 5a), more organized convection occurs over the Arabian Sea and the western equatorial Indian Ocean in P1, while suppressed convection occurs over the eastern Indian Ocean, the Maritime Continent and the western Pacific. The region of enhanced convection migrates from the western Indian Ocean to eastward and is located over the central Indian Ocean in P2, the eastern Indian Ocean in P3 and parts of the Maritime Continent in P4. During P2, P3 and P4, enhanced convection occurs over large portion of the BoB which is favorable for TC formation. Therefore, TC activity is significantly higher in these three MJO phases. The region of enhanced convection continuously propagates eastward from the Maritime Continent to the western Pacific in P5, while large portions of the North Indian Ocean (west of $\sim 90^\circ\text{E}$) experience suppressed convection. Less organized convection in P6 drives fewer TC formations in the BoB. In P6 and P7, strong positive anomalies (suppressed convection) occur over the entire North Indian Ocean, and the region of negative anomalies shifts eastward towards the central and eastern Pacific. The difference in OLR anomalies between P4 and P7 reaches 18 W m^{-2} (Table 2). No TCs have formed during P8 when enhanced convection occurred over the Western Hemisphere and Africa. The center of the convective anomalies is located south of the equator during AMJ.

The OLR anomaly patterns during OND are very similar to AMJ (Fig. 5b), although the center of the convective anomalies is positioned to the north of the equator. When enhanced convection occurs over the eastern Indian Ocean, the Maritime Continent and the western Pacific (P4 and P5), overall TC activity (particularly ACE and PDI) is significantly enhanced over the BoB in OND (Table 1). From P6 to P8, strong positive OLR anomalies (suppressed convection) prevail over the North Indian Ocean. The difference in OLR between phases 4 and 7 reaches $\sim 22 \text{ W m}^{-2}$ over the BoB (Table 2). This difference in OLR anomalies in the enhanced and suppressed phases is larger than other TC basins (Klotzbach, 2014), as MJO events tend to initiate and have a high amplitude over the Indian Ocean (Madden and Julian, 1972). The locations of cyclogenesis closely follow the migration of OLR anomalies in OND. During P2 and P3, most TCs form over the southwestern and southern parts of the BoB where the enhanced convection occurs (Fig. 4). The cyclogenesis locations shift slightly northward in P4 and P5 along with the migration of the enhanced convection region. These two phases are most favorable for TC genesis over the BoB, when the region of enhanced convection lies over the eastern Indian Ocean, the

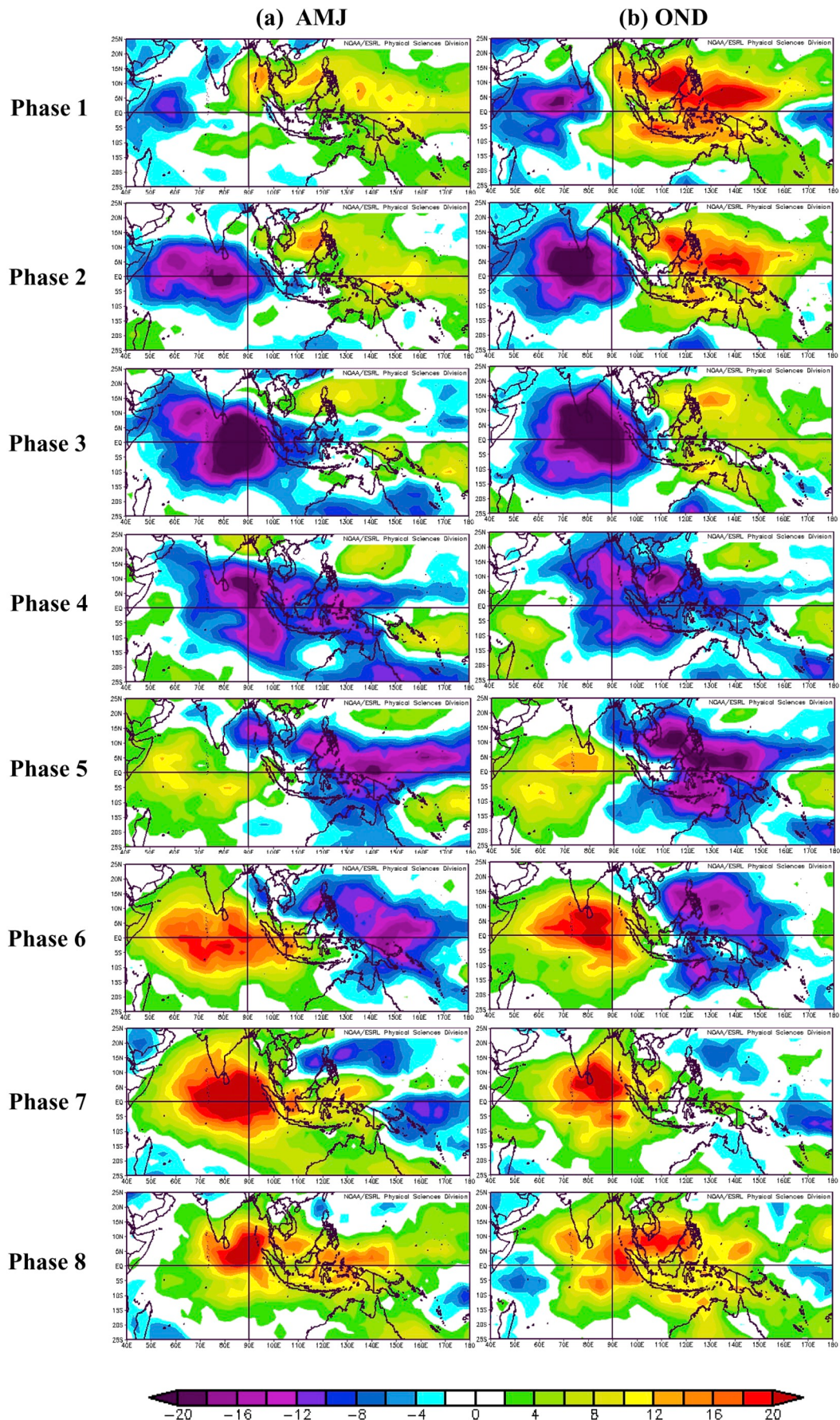


Fig. 5. OLR anomaly composites of (a) AMJ and (b) OND periods associated with each phase of the MJO.

Table 2

The averaged anomalous values of OLR (Wm^{-2}), 500 hPa RH (%), SSTA ($^{\circ}\text{C}$), SLP (hPa), 200 hPa, 850 hPa U, and the difference of 200 and 850-hPa U (e.g., zonal wind shear) by MJO phase for all days during AMJ and OND for the period 1974–2015. Anomalies are calculated from the 1981–2010 average. Anomalies are calculated over the BoB region ($5^{\circ}\text{--}22.5^{\circ}\text{N}$, $80^{\circ}\text{--}100^{\circ}\text{E}$). The values that are 95% significant in a positive (negative) manner for TCs are bold faced (italicized).

MJO Phase	OLR (Wm^{-2})	RH ₅₀₀ (%)	SSTA ($^{\circ}\text{C}$)	SLP (hPa)	U ₂₀₀ (ms^{-1})	U ₈₅₀ (ms^{-1})	U ₂₀₀ -U ₈₅₀ (ms^{-1})
AMJ							
1	5.80	−2.28	0.01	0.05	1.58	−0.92	2.51
2	−1.12	1.22	0.04	−0.18	1.68	−1.21	2.89
3	−6.69	2.49	0.13	−0.47	1.11	−0.84	1.96
4	−7.54	2.45	0.11	−0.89	−1.24	−0.09	1.14
5	−5.52	3.11	−0.05	−0.67	−2.40	1.09	−3.49
6	2.93	−0.58	−0.18	0.01	−1.57	1.69	−3.25
7	10.91	−4.22	−0.17	0.55	0.04	0.89	−0.93
8	10.81	−4.17	−0.09	0.56	0.80	−0.72	1.52
OND							
1	6.45	−3.10	−0.02	0.87	4.03	−1.63	5.66
2	−2.88	0.50	0.03	−0.20	2.99	−1.36	4.35
3	−9.77	2.28	0.10	−0.76	−0.96	−0.26	−0.70
4	−10.05	1.30	0.08	−0.90	−3.47	0.86	−4.33
5	−2.99	1.97	0.00	−0.68	−3.25	1.35	−4.60
6	6.58	−0.62	−0.02	0.01	−1.34	1.47	−2.81
7	11.78	−3.32	−0.17	0.84	1.65	0.07	1.58
8	9.42	−3.79	−0.18	0.90	2.60	−0.95	3.55

Maritime Continent and the western Pacific. During P6, TCs tend to form over the northeast part of the BoB as the enhanced convection shifts northeastward. The remaining three phases (P7-P8, P1) accounted for much less TC activity. No systematic pattern was observed in either TC genesis location or tracks over the BoB during these three phases. Overall, TC activity significantly increases in the BoB during and immediately after the enhanced convective phase.

3.4.2. Relative humidity (RH)

Mid-tropospheric RH is one of the key parameters triggering the development and intensification of TCs. A dry mid troposphere is unfavorable for the initiation and persistence of widespread deep convective activity (Gray, 1979). A mid-tropospheric RH of 40% is considered to be the minimum level necessary for TC formation (Gray, 1968, 1975). Camargo et al. (2009) observed that the MJO caused alterations in mid-tropospheric RH that significantly changed the potential for TC genesis. Fig. 6 displays mid-tropospheric (500 hPa) RH anomalies corresponding to the eight different MJO phases during AMJ and OND. Positive (negative) anomalies indicate higher (lower) RH at mid-tropospheric levels. The RH anomaly pattern is nearly identical to the OLR pattern, as the RH anomalies are significantly influenced by the passage of convectively-enhanced and suppressed MJO phases. Strong convective activity moistens the mid troposphere during the active MJO phase, whereas reduced convective activity dries the mid troposphere during the inactive MJO phase. Mid-tropospheric RH is significantly enhanced in P2-P5 due to heightened convective activity over the BoB (Table 2). Higher RH leads to an increase in the release of latent heat that is needed for TC formation and intensification. Lower mid-tropospheric RH inhibits TC activity in P6-P8.

3.4.3. Sea surface temperature anomalies (SSTAs)

SST significantly controls the formation and intensification of TCs (Kotal et al., 2009; Yu and McPhaden, 2011; Sebastian and Behera, 2015). The threshold value for the formation of TC is generally taken to be 26.5°C (Gray, 1975). The mean SST over the BoB is higher than the threshold value in each MJO phase (not shown). The magnitude of the SSTA difference between active and inactive MJO phases during AMJ and OND is approximately 0.25°C (Fig. 7 and Table 2). The SSTAs are

significantly positive (at the 95% confidence level) in P3 and P4 during both periods. The combination of both dynamic and thermodynamic conditions associated with positive SSTAs support TC formation in P3 and P4 over the BoB. Conversely, negative SSTAs are unfavorable for TC formation during P6-P8 over the BoB.

3.4.4. Sea level pressure (SLP)

Fig. 8 displays the SLP anomaly pattern during AMJ and OND for each MJO phase. Like RH anomalies and SSTAs, SLP anomalies also follow the MJO propagation. In P2-P4, lower pressures occur over the North Indian Ocean, which supports TC formation. In P5, the region of low pressure is located over the BoB and the western and central Pacific Ocean. The SLP is significantly lower over the BoB in P3-P5 during both periods (Table 2), supporting increased TC activity. The remaining four phases (P6-P8, P1) are characterized by higher SLPs over the entire North Indian Ocean which hinders TC formation, since it tends to be associated with more stable air and large-scale subsidence.

3.4.5. Low level winds (850 hPa)

Fig. 9 displays the low-level wind anomaly (850 hPa) pattern over the BoB and the surrounding region during each MJO phase. In P1-P2, anomalous easterly winds (significant at the 95% confidence level) prevail at lower levels over the BoB. These anomalous easterly winds weaken significantly during P3. Anomalous westerly winds prevail in P4-P6 over the BoB when the MJO favors convection over the Maritime Continent and the western Pacific. These anomalous westerly winds create anomalous low-level cyclonic vorticity which is favorable for the formation of TCs over the BoB (Krishnamohan et al., 2012). Despite the presence of low-level cyclonic vorticity, TCs tend to not form in P6 due to less convective activity, lower RH, higher SLP, negative SSTAs and higher VWS. Anomalous low-level westerly winds begin to weaken and are then replaced by anomalous low-level easterly winds in P7 and P8 when the active MJO phase is transitioning into the Western Hemisphere.

3.4.6. Upper level winds (200 hPa)

Fig. 10 displays the upper-level wind anomaly (200 hPa) pattern over the BoB and surrounding region during each MJO phase. The upper-level wind displays a nearly opposite pattern to the lower-level wind pattern. In P1 and P2, anomalous westerly winds (significant at the 95% confidence level) prevail at upper levels over the BoB. These anomalous westerly winds weaken significantly in P3 and are replaced by anomalous easterlies in P4-P6. These anomalous easterlies weaken and are then replaced by anomalous westerlies as the MJO progresses into P7 and P8. Anomalous easterlies counteract the prevailing upper-level westerlies that predominate over the BoB during the cyclone season and consequently reduce vertical wind shear (as shown in the next section).

3.4.7. Vertical wind shear (VWS; 200–850 hPa)

VWS plays an important role in TC development and intensification. Low VWS favors TC genesis, whereas high VWS inhibits TC genesis (Gray, 1968; DeMaria, 1996; Maloney and Hartmann, 2000b; Zehr, 2003). Fig. 11 displays the pattern of VWS over the North Indian Ocean and the surrounding region during each MJO phase. VWS over the BoB is low in P3-P6 when the convectively-enhanced MJO phase is located over the Maritime Continent and the western and central Pacific Ocean. The anomalous westerly winds in the lower troposphere and anomalous easterly winds in the upper troposphere counteract the prevailing zonal winds across the BoB which leads to a reduction in VWS. Conversely, higher VWS hinders TC development in the convectively-suppressed MJO phases (P1-P2 and P7-P8) over the BoB during both periods. The difference in VWS between convectively enhanced and suppressed MJO phases is quite strong ($\sim 10 \text{ ms}^{-1}$ or ~ 20 knots), consistent with Klotzbach (2014). This indicates that TC formation is high over the BoB in those MJO phases when the VWS is reduced and other environmental

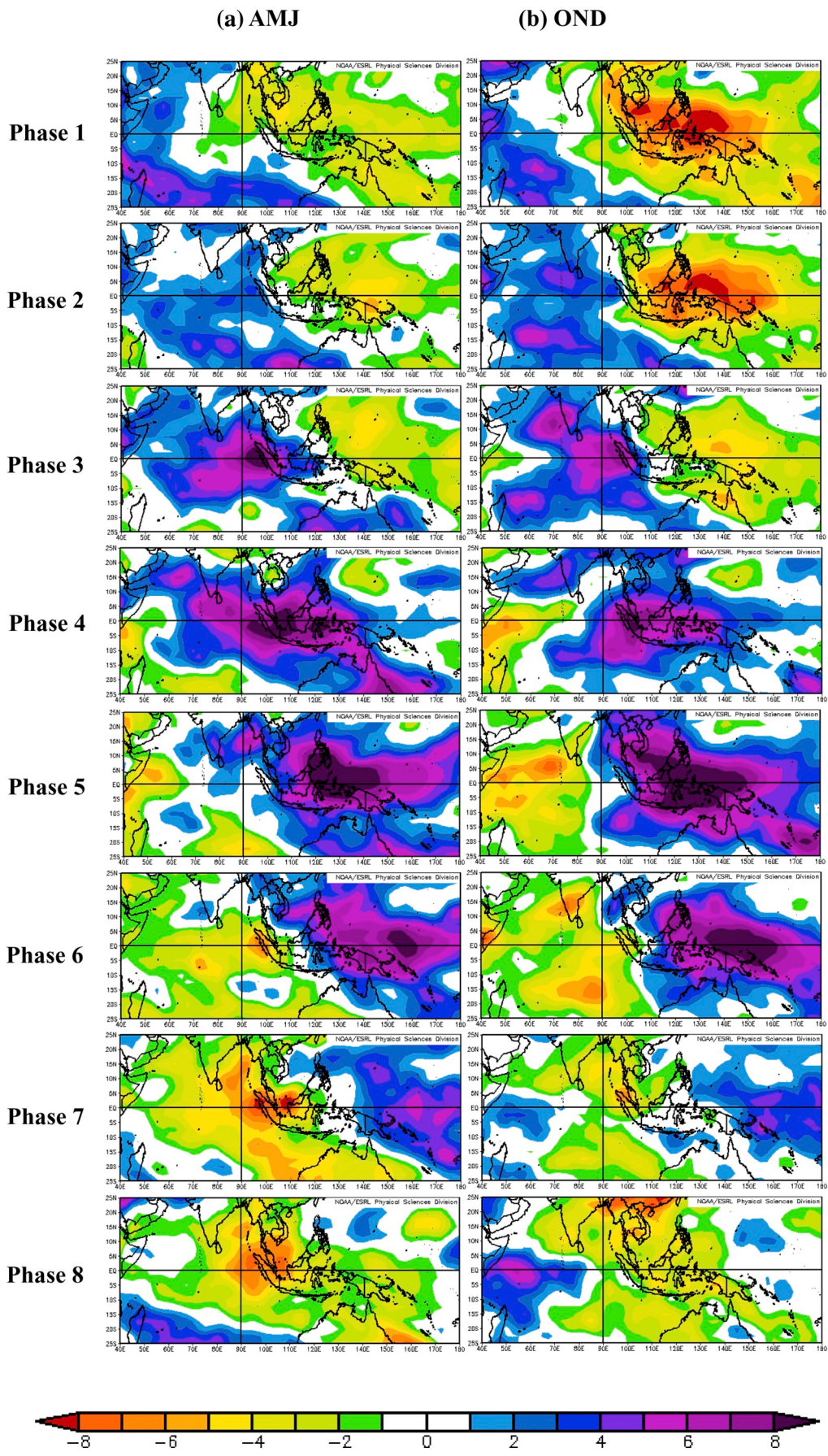


Fig. 6. As in Fig. 5, but for 500 hPa RH anomalies.

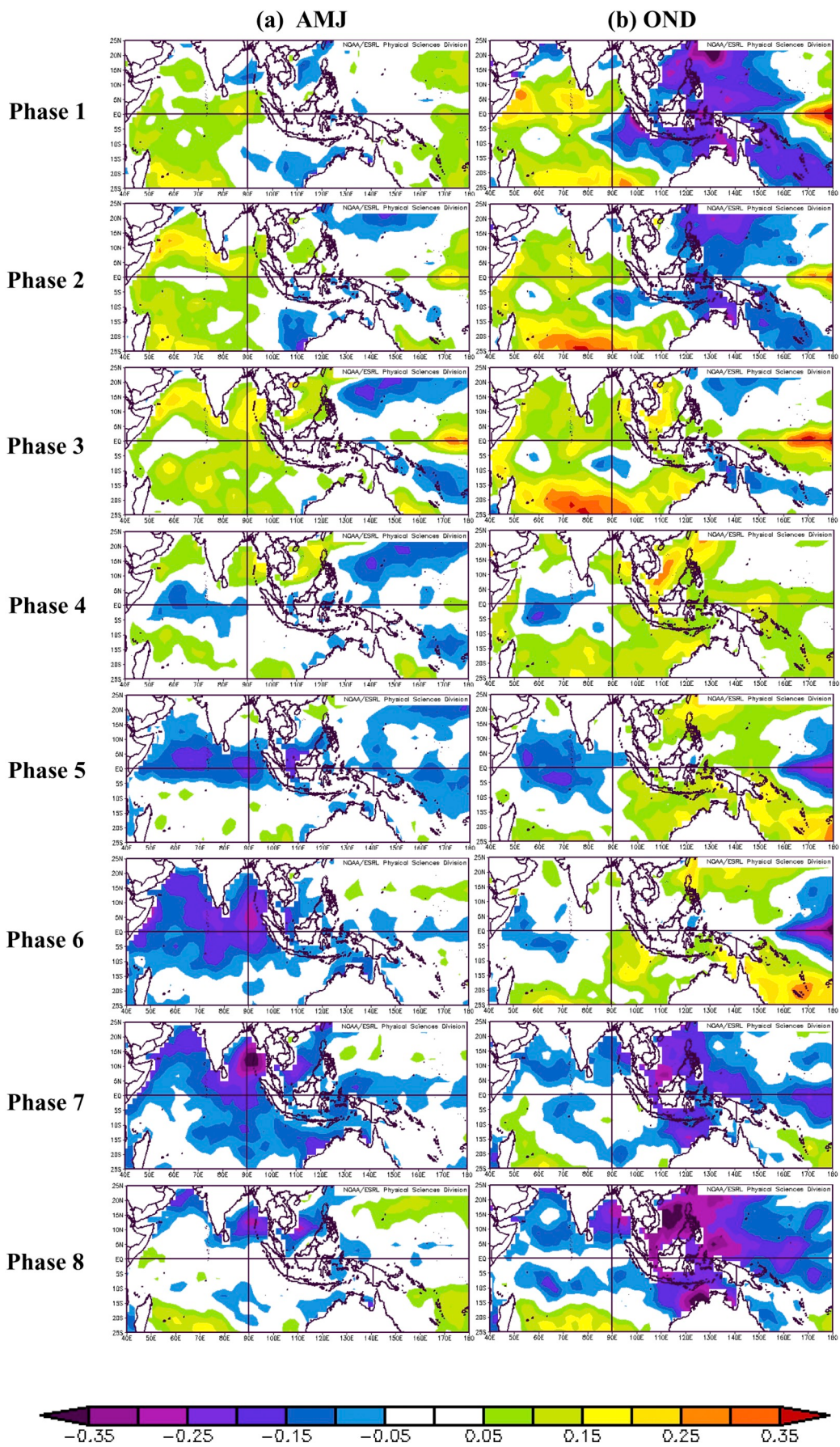


Fig. 7. As in Fig. 5, but for SSTAs.

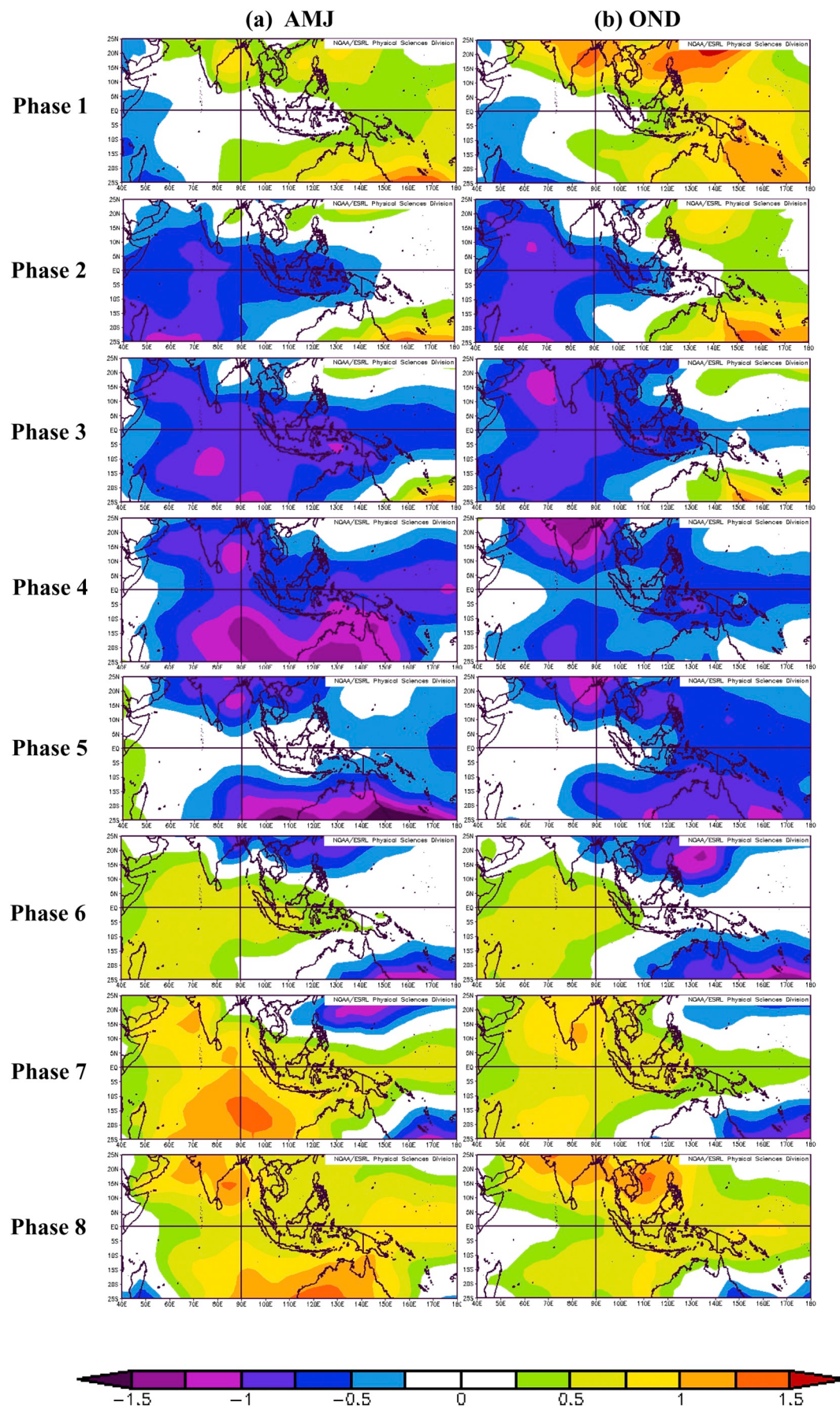


Fig. 8. As in Fig. 5, but for SLP anomalies.

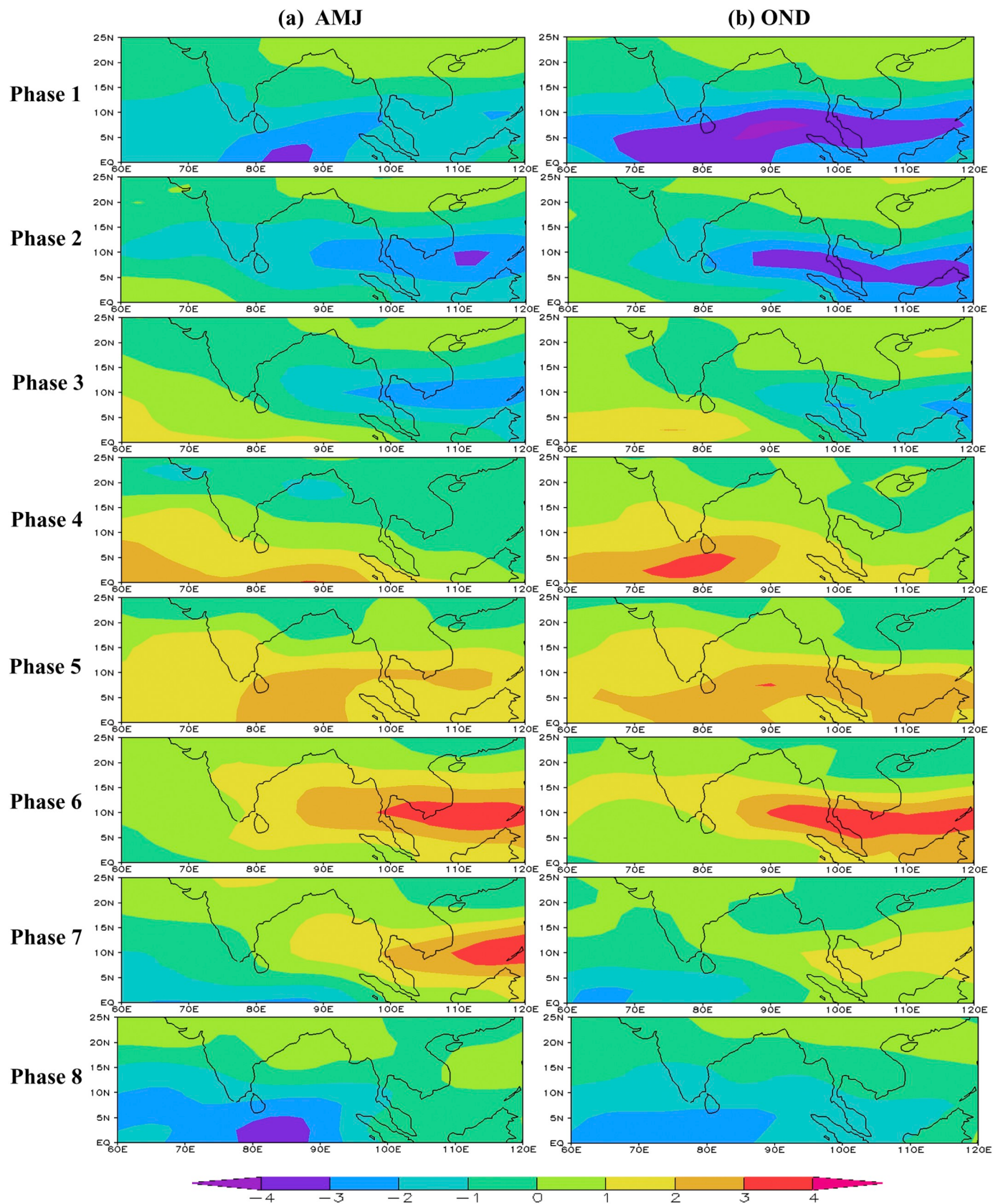


Fig. 9. As in Fig. 5, but for 850 hPa wind anomalies.

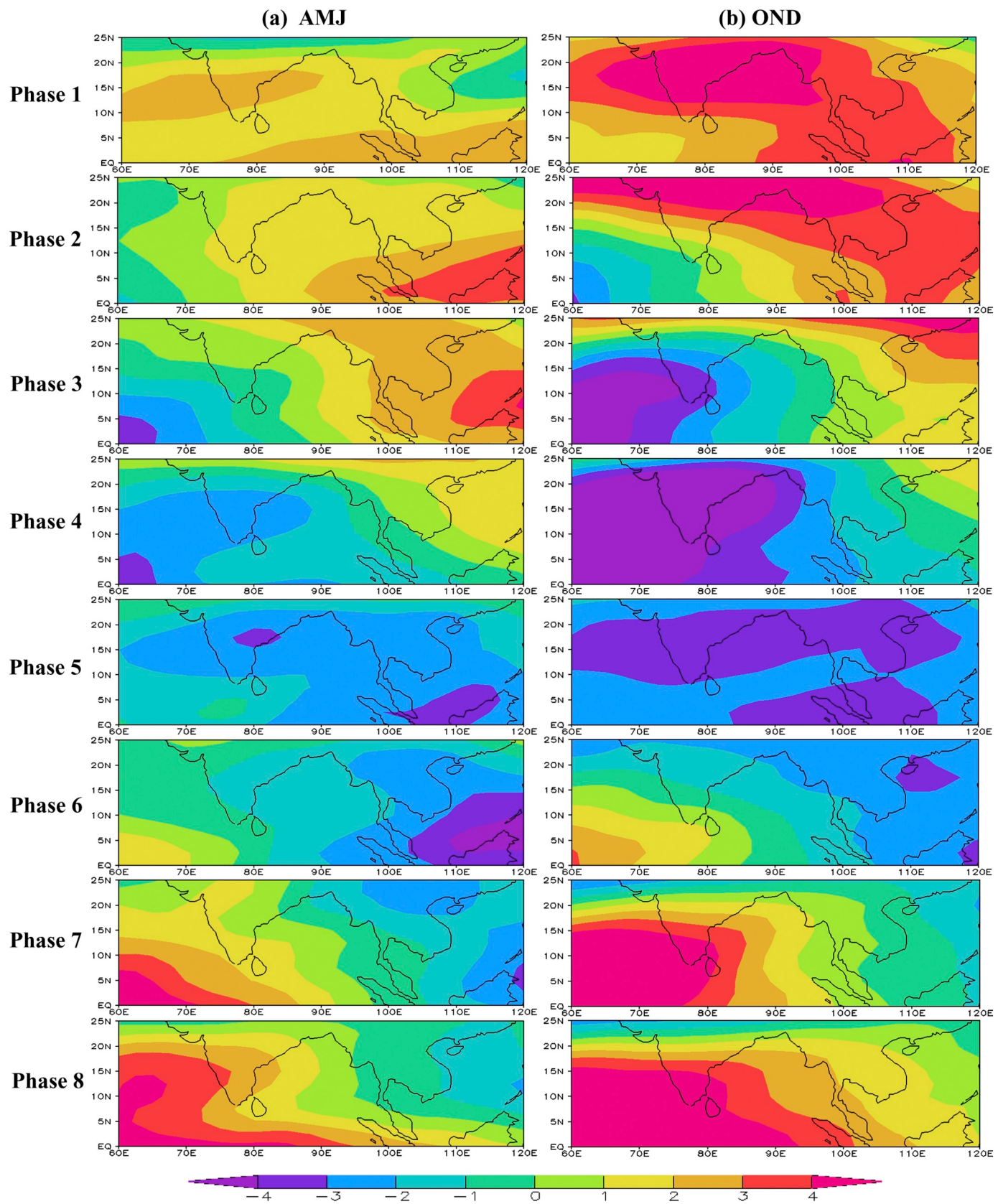


Fig. 10. As in Fig. 5, but for 200 hPa wind anomalies.

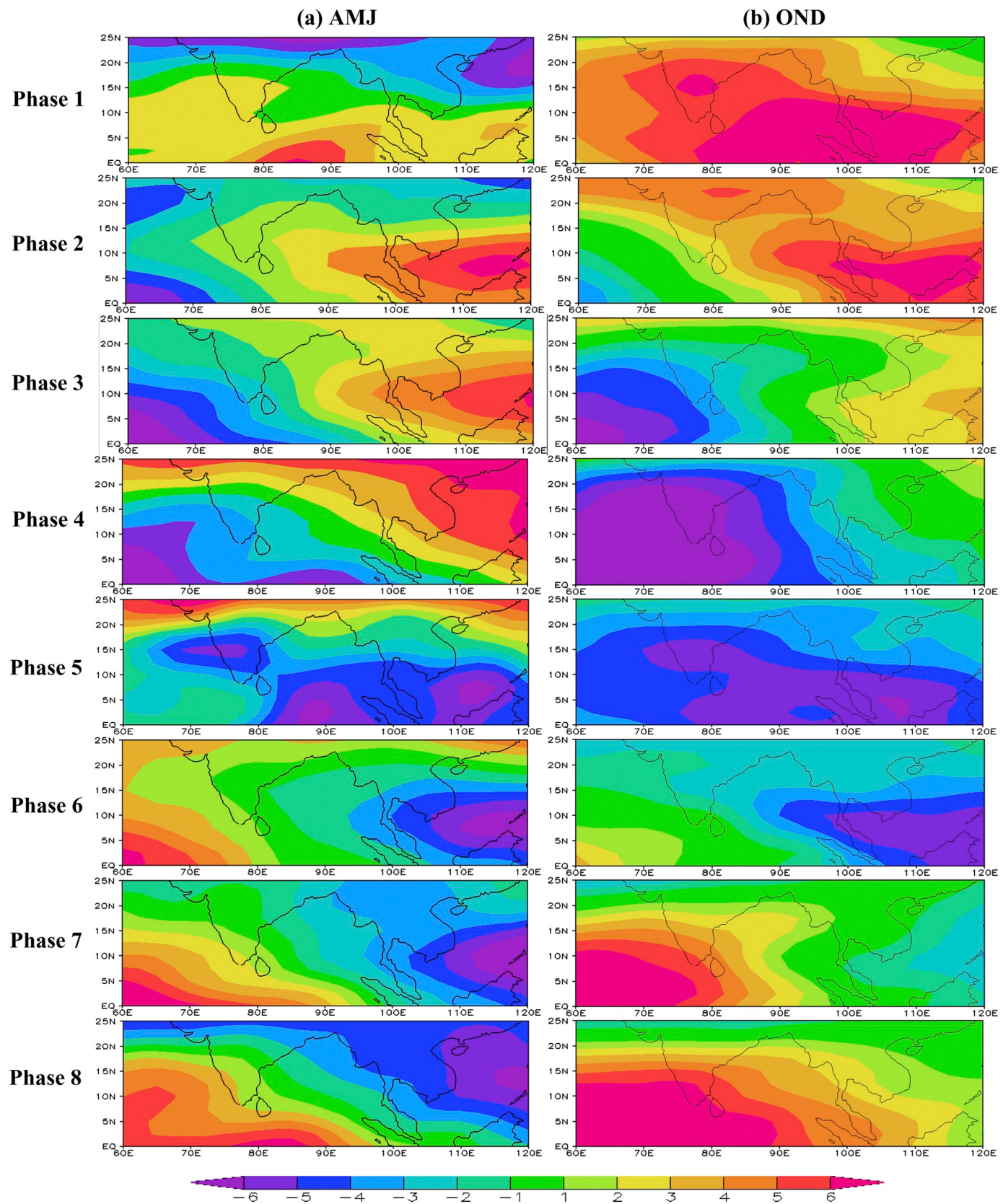


Fig. 11. As in Fig. 5, but for vertical wind shear (200–850 hPa).

conditions are also favorable for TCs.

4. Conclusions

In this study, we investigate the influence of the MJO (as defined by Wheeler and Hendon, 2004) on BoB TC activity during AMJ and OND for the period 1974–2015. The results of this study display a clear effect of the MJO on BoB TC activity. During AMJ, TC formation is significantly enhanced and suppressed over the BoB in P3-P4 and P8, respectively. Normalized ACE and PDI values are significantly higher in P2-P4 and lower in P7-P8. The MJO does not show a significant modulation of TC formation in OND; however, it does significantly modulate the duration of TCs and their ACE and PDI values. ACE and PDI values during OND are significantly enhanced in P2, P4-P5 and suppressed in P1, P7-P8. From this, it can be inferred that TC activity is significantly enhanced (suppressed) over the BoB when the convectively enhanced phase of the MJO is located over the eastern Indian Ocean, the Maritime Continent and the western Pacific (the Western Hemisphere and Africa). The genesis locations and tracks are also modulated by the MJO. These modulations in TC activity are mainly triggered by the MJO-driven alterations of large-scale oceanic and atmospheric conditions. Overall, the combination of more convective activity, higher RH, lower SLP, increased cyclonic vorticity, upper-level easterly winds and reduced VWS provide favorable conditions for TC formation and intensification in the BoB in P2-P5. Conversely, in phases 7–8, reduced convective activity, lower RH, higher SLP, anomalous upper-level westerly winds and higher VWS suppress TC activity over the BoB. Finally, the results of this study shed new light on the MJO-TC relationship which will improve the understanding of intraseasonal variability of TCs in the BoB.

Funding information

This research did not receive any specific grant from funding agencies in the public, commercial, or not-for-profit sectors.

Acknowledgements

The authors thank the anonymous reviewer for critical comments and constructive suggestions which improved the overall quality of the manuscript.

References

- Aiyyer, A., Molinari, J., 2008. MJO and tropical cyclogenesis in the Gulf of Mexico and eastern Pacific: case study and idealized numerical modeling. *J. Atmos. Sci.* 65, 2691–2704.
- Anandh, P.C., Vissa, N.K., Broderick, C., 2018. Role of MJO in modulating rainfall characteristics observed over India in all seasons utilizing TRMM. *Int. J. Climatol.* 38, 2352–2373.
- Barrett, B.S., Leslie, L.M., 2009. Links between tropical cyclone activity and Madden-Julian oscillation phase in the North Atlantic and Northeast Pacific basins. *Mon. Weather Rev.* 137, 727–744.
- Bell, G.D., Halpert, M.S., Schnell, R.C., Higgins, R.W., Lawrimore, J., Kousky, V.E., Tinker, R., Thiaw, W., Chelliah, W., Artusa, A., 2000. Climate assessment for 1999. *Bull. Am. Meteorol. Soc.* 81, 1328.
- Bessafi, M., Wheeler, M.C., 2006. Modulation of South Indian Ocean tropical cyclones by the Madden-Julian Oscillation and convectively coupled equatorial waves. *Mon. Weather Rev.* 134, 638–656.
- Bhardwaj, P., Pattanaik, D.R., Singh, O., 2019. Tropical cyclone activity over Bay of Bengal in relation to El Niño-Southern Oscillation. *Int. J. Climatol.* <https://doi.org/10.1002/joc.6165>.
- Bhatia, R., Singh, M., Pattanaik, D.R., 2017. Impact of Madden-Julian oscillation on onset of summer monsoon over India. *Theor. Appl. Climatol.* 128, 381–391.
- Camargo, S.J., Wheeler, M.C., Sobel, A.H., 2009. Diagnosis of the MJO modulation of tropical cyclogenesis using an empirical index. *J. Atmos. Sci.* 66, 3061–3074.
- Chand, S.S., Walsh, K.J.E., 2010. The Influence of the Madden-Julian Oscillation on tropical cyclone activity in the Fiji Region. *J. Clim.* 23, 868–886.
- Chen, J.M., Wu, C.H., Chung, P.H., Sui, C.H., 2018. Influence of intraseasonal-interannual oscillations on tropical cyclone genesis in the western North Pacific. *J. Clim.* 31, 4949–4961.
- Chowdhury, K.M.M.H., 2002. Cyclone preparedness and management in Bangladesh. In: BPATC (Ed.), *Improvement of Early Warning System and Responses in Bangladesh Towards Total Disaster Risk Management Approach*. BPATC, Savar, pp. 115–119 Dhaka.
- Chu, J.H., Sampson, C.R., Levine, A.S., Fukada, E., 2002. The Joint Typhoon Warning Center Tropical Cyclone Best-Tracks, 1945–2000. U.S. Naval Research Laboratory Report, pp. 22 NRL/MR/ 7540-02-16.
- DeMaria, M., 1996. The effect of vertical shear on tropical cyclone intensity change. *J. Atmos. Sci.* 53, 2076–2087.
- Efron, B., 1979. Bootstrap methods: another look at the jackknife. *Ann. Stat.* 7, 1–26.
- Emanuel, K.A., 2005. Increasing destructiveness of tropical cyclones over the past 30 years. *Nature* 436, 686–688.
- Frank, W.M., 1987. In: Elsberry, R.L. (Ed.), *A Global View of Tropical Cyclones*. Office of Naval Research, pp. 53–90 Tropical cyclone formation.
- Girishkumar, M.S., Suprit, K., Vishnu, S., Thanga Prakash, V.P., Ravichandran, M., 2015. The role of ENSO and MJO on rapid intensification of tropical cyclones in the Bay of Bengal during October–December. *Theor. Appl. Climatol.* 120, 797–810.
- Goswami, B.N., Ajayamohan, R.S., 2001. Intraseasonal oscillations and interannual variability of the Indian summer monsoon. *J. Clim.* 14, 1180–1198.
- Gray, W.M., 1968. Global view of the origin of tropical disturbances and storms. *Mon. Weather Rev.* 96, 669–700.
- Gray, W.M., 1975. Tropical Cyclone Genesis. Department of Atmospheric Science. Paper No. 234, Colorado State University, Fort Collins.
- Gray, W.M., 1979. Hurricanes: Their formation, structure and likely role in the tropical circulation. In: Shaw, D.B. (Ed.), *Meteorology over Tropical Oceans*, pp. 155–218 Royal Meteorological Society.
- Hall, J.D., Matthews, A.J., Karoly, D.J., 2001. The modulation of tropical cyclone activity in the Australian region by the Madden-Julian oscillation. *Mon. Weather Rev.* 129, 2970–2982.
- Ho, C.H., Kim, J.H., Jeong, J.H., Kim, H.S., Chen, D., 2006. Variation of tropical cyclone activity in the South Indian Ocean: El Niño Southern Oscillation and Madden Julian oscillation effects. *J. Geophys. Res.* 111, D22101.
- Huang, P., Chou, C., Huang, R., 2011. Seasonal modulation of tropical intraseasonal oscillations on tropical cyclone geneses in the western North Pacific. *J. Clim.* 24, 6339–6352.
- I.M.D., 2011. Tracks of Cyclones and Depressions over North Indian Ocean (from 1891 Onwards) (Cyclone eAtlas - IMD, Version 2.0). Cyclone Warning & Research Centre, India Meteorological Department, Regional Meteorological Centre, Chennai.
- Jones, C., Carvalho, L.M.V., 2002. Active and break phases in the South American Monsoon system. *J. Clim.* 15, 905–914.
- Jones, C., Carvalho, L.M.V., 2014. Sensitivity to Madden-Julian Oscillation variations on heavy precipitation over the contiguous United States. *Atmos. Res.* 147–148, 10–26.
- Kalnay, E., Kanamitsu, M., Kistler, R., Collins, W., Deaven, D., Gandin, L., Iredell, M., Saha, S., White, G., Woollen, J., Zhu, Y., Chelliah, M., Ebisuzaki, W., Higgins, W., Janowiak, J., Mo, K.C., Ropelewski, C., Wang, J., Leetmaa, A., Reynolds, R., Jenne, R., Joseph, D., 1996. The NCEP/NCAR 40-Year Reanalysis project. *Bull. Am. Meteorol. Soc.* 77, 437–471.
- Kikuchi, K., Wang, B., 2010. Formation of tropical cyclones in the northern Indian Ocean associated with two types of tropical intraseasonal oscillation modes. *J. Meteorol. Soc. Jpn.* 88, 475–496.
- Kim, J.H., Ho, C.H., Kim, H.S., Sui, C.H., Park, S.K., 2008. Systematic variation of summertime tropical cyclone activity in the western North Pacific in relation to the Madden-Julian Oscillation. *J. Clim.* 21, 1171–1191.
- Klotzbach, P.J., 2010. On the Madden-Julian Oscillation-Atlantic hurricane relationship. *J. Clim.* 23, 282–293.
- Klotzbach, P.J., 2012. El Niño-Southern Oscillation, the Madden-Julian Oscillation and Atlantic basin tropical cyclone rapid intensification. *J. Geophys. Res.* 117, D14104.
- Klotzbach, P.J., 2014. The Madden-Julian Oscillation's impacts on worldwide tropical cyclone activity. *J. Clim.* 27, 2317–2330.
- Klotzbach, P.J., Blake, E.S., 2013. North-central Pacific tropical cyclones: impacts of El Niño-Southern Oscillation and the Madden-Julian oscillation. *J. Clim.* 26, 7720–7733.
- Klotzbach, P.J., Oliver, E.C.J., 2015a. Variations in global tropical cyclone activity and the Madden-Julian Oscillation since the midtwentieth century. *Geophys. Res. Lett.* 42, 4199–4207.
- Klotzbach, P.J., Oliver, E.C.J., 2015b. Modulation of Atlantic basin tropical cyclone activity by the Madden-Julian Oscillation (MJO) from 1905 to 2011. *J. Clim.* 28, 204–217.
- Ko, K.-C., Hsu, H.-H., 2009. ISO modulation on the submonthly wave pattern and recurring tropical cyclones in the tropical western North Pacific. *J. Clim.* 22, 582–599.
- Kotal, S.D., Kundu, P.K., Roy Bhownik, S.K., 2009. An analysis of sea surface temperature and maximum potential intensity of tropical cyclones over the Bay of Bengal between 1981 and 2000. *Meteorol. Appl.* 16, 169–177.
- Krishnamohan, K.S., Mohanakumar, K., Joseph, P.V., 2012. The influence of Madden-Julian oscillation in the genesis of North Indian Ocean tropical cyclones. *Theor. Appl. Climatol.* 109, 271–282.
- Krishnamurti, T.N., Jayakumar, P.K., Sheng, J., Surgi, N., Kumar, A., 1985. Divergent circulations on the 30–50 day time scale. *J. Atmos. Sci.* 42, 364–375.
- Landsea, C.W., Bell, G.D., Gray, W.M., Goldenberg, S.B., 1998. The extremely active 1995 Atlantic hurricane season: Environmental conditions and verification of seasonal forecasts. *Mon. Weather Rev.* 126, 1174–1193.
- Li, R.C.Y., Zhou, W., 2013a. Modulation of western North Pacific tropical cyclone activity by the ISO. Part I: Genesis and intensity. *J. Clim.* 26, 2904–2918.
- Li, R.C.Y., Zhou, W., 2013b. Modulation of western North Pacific tropical cyclone activity by the ISO. Part II: tracks and landfalls. *J. Clim.* 26, 2919–2930.
- Li, R.C.Y., Zhou, W., 2018. Revisiting the intraseasonal, interannual and interdecadal variability of tropical cyclones in the western North Pacific. *Atmospheric and Oceanic*

- Science Letters 11, 198–208.
- Li, R.C.Y., Zhou, W., Chan, J.C.L., 2012. Asymmetric modulation of Western North Pacific cyclogenesis by the Madden-Julian Oscillation under ENSO conditions. *J. Clim.* 24, 5374–5385.
- Liebmann, B., Hendon, H.H., Glick, J.D., 1994. The relationship between tropical cyclones of the western Pacific and Indian Oceans and the Madden-Julian Oscillation. *J. Meteorol. Soc. Jpn.* 72, 401–412.
- Lorenz, D.J., Hartmann, D.L., 2006. The effect of the MJO on the north American Monsoon. *J. Clim.* 19, 333–343.
- Madden, R.A., Julian, P.R., 1971. Detection of a 40–50 day oscillation in the zonal wind in the tropical Pacific. *J. Atmos. Sci.* 28, 702–708.
- Madden, R.A., Julian, P.R., 1972. Description of global-scale circulation cells in the tropics with a 40–50 day period. *J. Atmos. Sci.* 29, 1109–1123.
- Madden, R.A., Julian, P.R., 1994. Observations of the 40–50-day tropical oscillation—a review. *Mon. Weather Rev.* 122, 814–837.
- Maloney, E.D., Dickinson, M.J., 2003. The intraseasonal oscillation and the energetics of summertime tropical western North Pacific synoptic-scale disturbances. *Journal of Atmospheric Sciences* 60, 2153–2168.
- Maloney, E.D., Hartmann, D.L., 2000a. Modulation of hurricane activity in the Gulf of Mexico by the Madden-Julian oscillation. *Science* 287, 2002–2004.
- Maloney, E.D., Hartmann, D.L., 2000b. Modulation of eastern North Pacific hurricanes by the Madden-Julian oscillation. *J. Clim.* 13, 1451–1460.
- Mandalapaka, P.V., Qin, X., Lo, E.Y.M., 2017. Analysis of spatial patterns of daily precipitation and wet spell extremes in Southeast Asia. *Int. J. Climatol.* 37, 1161–1179.
- Maru, E., Shibata, T., Ito, K., 2018. Statistical analysis of tropical cyclones in the Solomon Islands. *Atmosphere* 9, 227. <https://doi.org/10.3390/atmos9060227>.
- Marzuki, Hashiguchi, H., Kozu, T., Shimomai, T., Shibagaki, Y., Takahashi, Y., 2016. Precipitation microstructure in different Madden-Julian Oscillation phases over Sumatra. *Atmos. Res.* 168, 121–138.
- Matthews, A.J., 2000. Propagation mechanisms for the Madden-Julian oscillation. *Q. J. R. Meteorol. Soc.* 126, 2637–2651.
- McBride, J.L., Zehr, R., 1981. Observational analysis of tropical cyclone formation. Part II: Comparison of non-developing versus developing systems. *J. Atmos. Sci.* 38, 1132–1151.
- Merrill, R.T., 1988. Environmental influences on hurricane intensification. *J. Atmos. Sci.* 45, 1678–1687.
- Mo, K.C., 2000. The association between intraseasonal oscillations and tropical storms in the Atlantic basin. *Mon. Weather Rev.* 128, 4097–4107.
- Molinari, J., Vollaro, D., 2000. Planetary- and synoptic-scale influences on eastern Pacific tropical cyclogenesis. *Mon. Weather Rev.* 128, 3296–3307.
- Molinari, J., Knight, D., Dickinson, M., Vollaro, D., Skubis, S., 1997. Potential vorticity, easterly waves, and eastern Pacific tropical cyclogenesis. *Mon. Weather Rev.* 125, 2699–2708.
- Nakazawa, T., 1986. Intraseasonal variation of OLR in the tropics during the FGGE year. *J. Meteorol. Soc. Jpn.* 64, 17–34.
- Neumann, C.J., 1993. Global overview. In: Holland, G.J. (Ed.), *Global Guide to Tropical Cyclone Forecasting*. World Meteorological Organization, Geneva, Report No. TCP-31, 1.1–1, pp. 56.
- Notaro, M., 2018. Enhancement of vegetation-rainfall feedbacks on the Australian summer monsoon by the Madden-Julian Oscillation. *Clim. Dyn.* 51, 3093–3109.
- Pattanaik, D.R., Rama Rao, Y.V., 2009. Track prediction of very severe cyclone “Nargis” using high resolution weather research forecasting (WRF) model. *Journal of Earth System Science* 118, 309–329.
- Ramsay, H.A., Camargo, S.J., Kim, D., 2012. Cluster analysis of tropical cyclone tracks in the Southern Hemisphere. *Clim. Dyn.* 39, 897–917.
- Sebastian, M., Behera, M.R., 2015. Impact of SST on tropical cyclones in North Indian Ocean. *Procedia Engineering* 116, 1072–1077.
- Shao, X., Li, S., Liu, N., Song, J., 2018. The Madden-Julian oscillation during the 2016 summer and its possible impact on rainfall in China. *Int. J. Climatol.* 38, 2575–2589.
- Sobel, A.H., Maloney, E.D., 2000. Effect of ENSO and MJO on the western North Pacific tropical cyclones. *Geophys. Res. Lett.* 27, 1739–1742.
- Thompson, D.B., Roundy, P.E., 2013. The relationship between the Madden-Julian Oscillation and U.S. violent tornado outbreaks in the spring. *Mon. Weather Rev.* 141, 2087–2095.
- Tsuboi, A., Takemi, T., 2014. The interannual relationship between MJO activity and tropical cyclone genesis in the Indian Ocean. *Geoscience Letters* 1, 9.
- Ventrice, M.J., Thorncroft, C.D., Roundy, P.E., 2011. The Madden-Julian oscillation's influence on African easterly waves and downstream tropical cyclogenesis. *Mon. Weather Rev.* 139, 2704–2722.
- Wang, B., Moon, J.Y., 2017. An anomalous genesis potential index for MJO modulation of tropical cyclones. *J. Clim.* 30, 4021–4035.
- Wang, B., Moon, J.Y., 2017a. Sub-seasonal prediction of extreme weather events. In: Chung, C.S., Wang, B. (Eds.) *Bridging Science and Policy Implication for Managing Climate Extremes: Linking Science and Policy Implication*. World Scientific, in press.
- Wheeler, M.C., Hendon, H.H., 2004. An all-season real-time multivariate MJO index: development of an index for monitoring and prediction. *Mon. Weather Rev.* 132, 1917–1932.
- Yu, L., McPhaden, M.J., 2011. Ocean preconditioning of cyclone Nargis in the Bay of Bengal: Interaction between Rossby waves, surface fresh waters, and sea surface temperatures. *J. Phys. Oceanogr.* 41, 1741–1755.
- Zaitchik, B.F., 2017. Madden-Julian Oscillation impacts on tropical African precipitation. *Atmos. Res.* 184, 88–102.
- Zehr, R.M., 2003. Environmental vertical wind shear with hurricane Bertha (1996). *Weather Forecast* 18, 345–356.
- Zhang, C., 2005. Madden-Julian Oscillation. *Rev. Geophys.* 43, RG2003.
- Zhao, H., Yoshida, R., Raga, G.B., 2015. Impact of the Madden-Julian Oscillation on Western North Pacific tropical cyclogenesis associated with large-scale patterns. *J. Appl. Meteorol. Climatol.* 54, 1413–1429.
- Zhou, W., Chan, J.C.L., 2005. Intraseasonal Oscillations and the South China Sea summer monsoon onset. *Int. J. Climatol.* 25, 1585–1609.